ISSN 0023-1584, Kinetics and Catalysis, 2011, Vol. 52, No. 6, pp. 798–804. © Pleiades Publishing, Ltd., 2011.
Original Russian Text © B.E. Krisyuk, A.V. Maiorov, 2011, published in Kinetika i Kataliz, 2011, Vol. 52, No. 6, pp. 819–825.

Quantum Chemical Study of the Primary Step of Ozone Addition at the Double Bond of Ethylene

B. E. Krisyuk[a,*] and A. V. Maiorov[b,]**

[a] *Institute of Problems of Chemical Physics, Russian Academy of Sciences, Chernogolovka, Moscow oblast, 142432 Russia*
[b] *Emanuel Institute of Biochemical Physics, Russian Academy of Sciences, Moscow, 117977 Russia*
*e-mail: * bkris@mail.ru, ** hruk@list.ru*

Received February 25, 2011

Abstract—The mechanism of the primary step of the interaction between ozone and the double bond of ethylene has been investigated by various methods of quantum chemistry (MP2, QCISD, CCSD, MRMP2) and density functional theory (PBE0, OPTX, CPW91, B3PW91, OLYO, B3LYP, BLYP). The kinetics of two reaction pathways, namely, concerted ozone addition via a symmetric transition state (Criegee mechanism) and nonconcerted ozone addition via a biradical transition state (DeMore mechanism) has been calculated. Both mechanisms are describable well in the single-determinant approximation by the QCISD, CCSD, B3LYP, and PBE0 methods and in the multideterminant approximation by the MRMP2 method. The other methods are less suitable for solving this problem. The calculated data demonstrate that the reaction proceeds via both competing pathways. Rate constant values consistent with experimental data and plausible Criegee-to-DeMore rate constant ratios have been obtained. The concerted addition of ozone to ethylene is significantly more rapid than the nonconcerted addition.

DOI: 10.1134/S0023158411060103

The interaction between ozone and the double bond is among the most specific reactions of unsaturated organic compounds. In recent decades, the mechanism of this reaction has been extensively investigated both theoretically and experimentally [1–3].

It was believed until recently that this reaction occurs via 1,3-cycloaddition through the formation of a symmetric transition state (TS1) to yield a five-atom cyclic molozonide, or primary ozonide, in its first step (Criegee mechanism [4]):

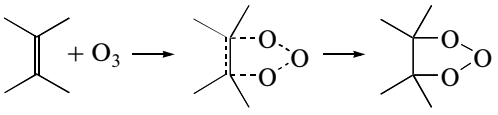

This scheme was verified by numerous direct and indirect experimental data [1, 2].

The alternative mechanism, according to which ozone interacts with the double bond like a peroxyl radical, yielding a biradical transition state (TS2), was suggested by DeMore [5] to account for the observed Arrhenius parameters of the reaction between ozone and acetylene:

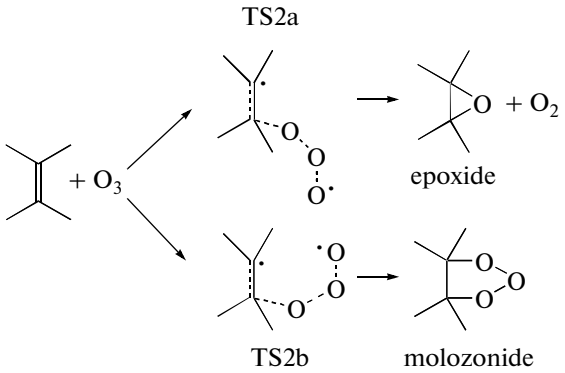

Later, after this reaction was studies in greater detail by contemporary quantum chemical methods, DeMore's mechanism was abandoned [6]. However, this mechanism explains the formation of oxides and aldehydes by molozonide decomposition. In addition, there are other arguments in favor of this mechanism [7].

In most theoretical works, the mechanism of the reaction examined was analyzed using the restricted Hartree–Fock (RHF) or restricted Kohn–Sham method. However, the ground state of ozone is the superposition of a zwitterion and a biradical. In the latter, the unpaired electrons are at the terminal oxygen atoms [8]. The contribution from the biradical to the resonance structure is about 59% [9]. The most

appropriate approach to solving quantum problems for such systems is the unrestricted Hartree–Fock (UHF) method [10], and the difference between the energies calculated by the RHF and UHF methods can served as a measure of the biradical nature of ozone.

UHF calculations demonstrated that the reaction can also proceed as nonconcerted addition via the formation of TS2 [11]. The above pathways of the reactions of ozone with ethylene and propylene were studied by single-determinant methods [12], and it was shown that these compounds prefer the Criegee pathway. However, the competition between the Criegee and DeMore mechanisms depends on the surroundings of the double bond: the reaction between ozone and ethylene occurs mainly via the Criegee mechanism [13], the reactions of ozone with tetrafluoroethylene and hexafluoropropylene are dominated by the DeMore mechanism [14, 15], and acetylene ozonation proceeds via both mechanism in comparable proportions [16]. The results of these quantum chemical calculations [13–16] were verified by the intersecting-parabolas semiempirical method [7]. It was demonstrated in the above-cited works that TS1 is detectable by ab initio and RHF calculations; TS2, by UHF calculations. It has become possible to describe both transition states at one level only by using the DFT UB3LYP method.

However, use of a single computational method yields insufficiently reliable results. The purpose of this study was to verify the earlier data by other quantum chemical methods and to see, by examining the reaction between ozone and ethylene, which of these methods are suitable for describing the interaction of ozone with multiple bonds of organic compounds. Ethylene ozonation can be considered as a test reaction since it has been investigated in detail. For example, the rate constant of this reaction in the gas phase is known to be $k = 10^3$ l mol^{-1} s^{-1} [17], the activation energy is approximately 20 kJ/mol, and the reaction occurs mainly via the Criegee mechanism. For single-determinant methods, an additional data reliability criterion is a nonzero value of the squared spin S^2 for ozone and TS2, which is an indication of the biradical nature of ozone.

COMPUTATIONAL METHODS

Calculations were carried out at the Computational Center of the Institute of Problems of Chemical Physics, Russian Academy of Sciences (Chernogolovka, Moscow oblast), using the GAUSSIAN-03 [18], US GAMESS Version 7 [19], and PC GAMESS Version 7.0 [20] programs for both closed and open shells (for restricted and unrestricted Hartree–Fock and Kohn–Sham methods). Basis sets of the 6-31G/6-311G family with diffuse functions, cc-PVDZ(PVTZ), and aug-cc-PVDZ(PVTZ) were employed. The parameters of the states corresponding to potential energy surface minima were determined with full optimization of all variables. The transition state was located using the geometries of states lying before and after the TS along the reaction coordinate. Normal vibration frequencies were calculated at the extremum points of the potential energy surface. MCSCF and MRMP2 multi-configuration calculations were carried out using the geometry of a given state at the MP2/UMP2, UB3LYP, or CASSCF level. Many of these methods are dimensionally inconsistent. For these methods, we scanned the reaction coordinate on both sides of the transition state. Once the energy plateaued at large coordinates, with the distance between the reacting atoms being 2.5–4.0 Å, scanning was sopped, and the energy thus determined was taken to be energy of the reactants. The size of the active space for ethylene was described as (2, 2): two electrons on two orbitals (bonding and antibonding π orbitals). For ozone, the active space (n, m), where n is the number of electrons and m is the number of orbitals, was varied between (2, 2) and (10, 10) or (12, 9) in order to determine the minimum(n, m) size for the given problem. Various active spaces were considered for ozone in the literature. The best substantiated active space sizes are (8, 7) and (12, 9) [21–23]. The corresponding space sizes for the reactant complexes and transition states are (10, 9) and (14, 11).

The enthalpy and entropy of the reaction were calculated using the results of the quantum chemical calculations and Ignatov's program MOLTRAN [24]. The rate constants of the reaction were calculated in terms of standard transition state theory using the results of the quantum chemical and thermodynamic calculations.

RESULTS AND DISCUSSION

Calculations for the interaction between ozone and the double bond of ethylene in the single-determinant approximation (Table 1) demonstrated that, along with UB3LYP, QCISD and CCSD are also suitable for this purpose. With UHF theory, these methods (UQCISD and UCCSD) lead to $S^2 = 0.35$ and 0.2, respectively. After triplet annihilation, this quantity becomes nearly zero in both cases.

Unfortunately, computational programs that could optimize the geometry within the MRMP2 method are unavailable for the authors. For this reason, the multi-configuration calculations of transition states in this work were performed in the following three ways: (1) TS geometry was optimized by the UMP2 method, thereafter the reaction coordinate was scanned at the CASSCF level, and then the MRMP2 energy was cal-

Table 1. Ozone state parameters calculated by single-determinant methods

Method	Basis set	E[a], Ha	Parameter[b]			
			R_{OO}, Å	α, deg	S^2	S^2A
QCISD	6-31+g**	−224.8632605	1.28	117.63	0	0
	6-311g**	−224.954454	1.26	117.65	0	0
	6-311+g**	−224.967131	1.26	117.96	0	0
	aug-cc-PVDZ	−224.935873	1.26	117.4	0	0
UQCISD	6-31+G**	−224.8661987	1.28	118.14	0.42	0.07
	6-311G**	−224.9567194	1.26	118.25	0.35	0.04
	6-311+G**	−224.9694718	1.26	118.51	0.35	0.04
	aug-cc-PVDZ	−224.9381457	1.27	117.98	0.34	0.04
CCSD	aug-cc-PVDZ	−224.9318885	1.26	117.26	0	0
UCCSD	aug-cc-PVDZ	−224.9316209	1.26	117.04	0.20	0.01

[a] Total electron energy.
[b] R_{OO} = O–O bond length, α = bond angle, S^2 = squared spin operator, and S^2A = S^2 value after annihilation.

culated at each point of the resulting curve; (2) TS geometry optimization and reaction coordinate scanning were carried out by the CASSCF method, and further calculations were performed as in procedure (1); (3) TS geometry optimization and reaction coordinate scanning were carried out by the B3LYP (UB3LYP) method, and further calculations were performed as in procedure (1).

Calculations for the reactants were performed in the same way, but without scanning the reaction coordinate. The results of the multi-configuration calculations for ozone are presented in Table 2. Clearly, at fairly large active spaces (starting at (8, 7)), all methods yield similar results. The energy of ozone calculated via procedures (1) and (3) is slightly higher than the ozone energy calculated via procedure (2). Therefore, the active space in multi-configuration calculations should not smaller than (8, 7) and that procedure (2) is somewhat more suitable for the problem considered. For this reason, we will mainly use procedure (2).

Table 2. Ozone energy calculated by the multi-configuration method MRMP2 using different active space sizes

(n, m)	E, Ha		
	procedure (1)	procedure (2)	procedure (3)
(2, 2)	−224.8729710	−224.8731615	–
(4, 4)	−224.8659902	−224.8761621	–
(6, 6)	−224.8803130	−224.8753402	–
(8, 7)	–	−224.8730422	−224.8711799
(8, 8)	−224.8695733	−224.8693691	–
(10, 10)	−224.8725406	−224.8704844	–
(12, 9)	–	−224.8771808	−224.8765730

Figure 1 shows typical curves obtained by scanning the reaction coordinate. These curves are monotonic, without any outliers. The activation energy at the CASSCF level is 90–120 kJ/mol, depending on the reaction mechanism. With the MP2 corrections taken into account it takes smaller values of 25 and 40 kJ/mol for the Criegee and DeMore mechanisms, respectively. The curves (both with and without MP2 corrections applied) show no minimum at large reaction coordinates, suggesting that there is a weakly bonded complex. This seems to be due to the incomplete optimization of the TS geometry by the above methods, because of which the complex is merely missed. Note that the geometry is optimized at the MCSCF or B3LYP level, while the energy is calculated at the MRMP2 level. Note also that the total energy of the initial compounds is substantially higher (by 2.3, 21.5, and 50 kJ/mol with the UB3LYP, CASSCF, and MRMP2 methods, respectively) than the energy of the reactants separated by a fairly long distance (3–4 Å). As a consequence, the rate constant calculated by the conventional method without scanning the reaction coordinate, based on the TS energy and the total energy of the initial compounds, is considerably overestimated.

The calculated TS energies and rate constants are listed in Tables 3–5. The structure of TS 1 was multiply analyzed earlier [25]. It is characterized by equally long C...O distances (R_{CO}) in each pair of atoms. The R_{CO} values calculated by the MP2, CCSD, QCISD, and B3LYP methods are 1.97, 2.2, 2.2, and 2.3 Å,

respectively. Two TS2 configurations are possible (see above), which differ in the position of the ozone moiety relative to the double bond (Fig. 2): *trans* configuration (TS2a) and *cis* configuration (TS2b). Note that the existence of TS2a is confirmed at all computational levels, while TS2b is not always detectable. This is likely due to the fact that, during the optimization of the *cis* TS, the program may "fall down" to TS1, in which the energy of ethylene is significantly lower. Note also that TS2a and TS2b are similar in energy, the *cis* TS2 configuration being only slightly more preferable, so all inferences will be the same for both of them.

Table 3 presents the data calculated by different DFT methods, which are comparatively undemanding of computational resources. At the same time, they satisfactorily describe electronically very different objects, such as TS1 and TS2. It follows from the data listed in Table 3 that the activation energies and rate constants are satisfactorily described by the methods involving hybrid functionals. The best fits to experimental data are provided by the B3LYP and PBE0 methods. In the UB3LYP calculations (as well as in the MPMP2 calculations, see above), the total energy of the initial compounds is 2.3 kJ/mol higher than the energy of the reactant separated by a distance of 3.5–4 Å. Even with this circumstance taken into account, the UB3LYP method yields somewhat underestimated values of TS1 energy and, accordingly, activation energy, so the rate constant k_1 is overestimated,

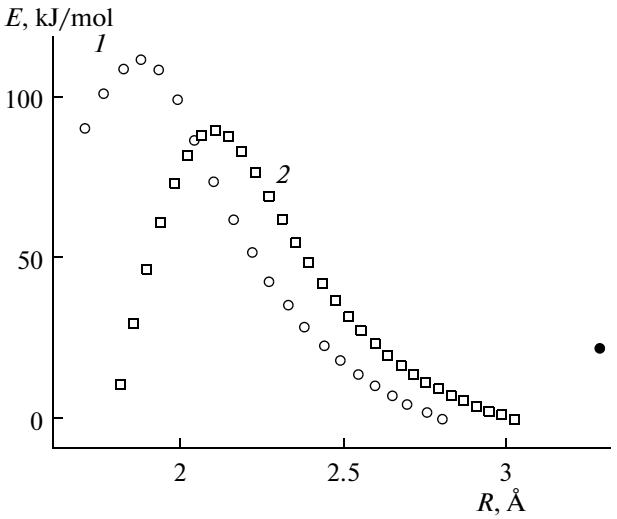

Fig. 1. Ethylene + ozone system energy E versus the reaction coordinate (scanning data) for the reaction proceeding via the (*1*) Criegee mechanism (TS1) and (*2*) DeMore mechanism (TS2). The calculation was carried out by the CASSCF(14, 11)/6-31+G** method. The black point indicates the total energy of the initial compounds, which differs from the energy of the separated reactants by E_0.

Table 3. TS parameters calculated using DFT methods

Method	Basis set	TS type	E[a], Ha	Parameter[b]		
				E_a, kJ/mol	$k \times 10^3$ at 298 K, l mol^{-1} s^{-1}	k_1/k_2
B3LYP	6-31+G**	TS1,	−304.02165	2.9	37.6	120
		TS2, $S^2 = 0.7$	−304.01406	22.8	0.31	
	aug-cc-PVDZ	TS1	−304.0581499	5.9	2.94	184
		TS2, $S^2 = 0.7$	−304.0500496	27.17	0.016	
PBE0	aug-cc-PVDZ	TS1	−303.7181891	6.65	7.88	81
		TS2, $S^2 = 0.7$	−303.7109986	25.53	0.097	
B3PW91	aug-cc-PVDZ	TS1	−303.9357123	3.81	24.7	452
		TS2, $S^2 = 0.67$	−303.9271229	26.36	0.055	
BLYP	aug-cc-PVDZ	TS1	−304.0273017	1.04	85	4326
		TS2, $S^2 = 0.4$	−304.0156427	26.86	0.020	
OLYP	aug-cc-PVDZ	TS1	−303.9975439	19.43	0.028	7025
		TS2, $S^2 = 0.4$	−303.98667	47.98	4×10^{-6}	
OPTX	aug-cc-PVDZ	TS1	−302.6111996	55.67	7×10^{-9}	0.18
		TS2, $S^2 = 0.7$	−302.6083553	63.14	4×10^{-8}	
CPW91	aug-cc-PVDZ	TS1	−303.7691334	30.22	7×10^{-5}	26
		TS2, $S^2 = 1.145$	−303.8150014	49.33	2.7×10^{-6}	

[a] Total energy.
[b] S^2 = squared spin operator for TS2, E_a = activation energy, k = overall rate constant including the rate constants of the Criegee (k_1) and DeMore (k_2) mechanisms.

Table 4. TS parameters calculated by ab initio methods

Method	Basis set	TS type	E, Ha	Parameter[a]		
				E_a, kJ/mol	$k \times 10^3$, $l\,mol^{-1}\,s^{-1}$	k_1/k_2
UMP2	6-31+G**	TS1	−303.20415	13.76	4.57	
		TS2, $S^2 = 1.2$	(-303.12843) −303.12770	(212.57) 214.47	–	
	cc- PVTZ	TS1	−303.51482	9.09	19.0	
		TS2, $S^2 = 1.2$	(−303.43568)	(216.86)	–	
	aug-cc-PVDZ	TS1	−303.28635	0.81	758	
		TS2, $S^2 = 1.2$	(−303.20673)	(209.86)	–	
UQCISD	6-31+G**	TS1	−303.20732	26.98	0.00299	1.78
		TS2, $S^2 = 1.2$	(−303.20424)	(35.07)	0.00168	
	aug-cc-PVDZ	TS1	−303.28927	19.54	0.0503	5.69
		TS2, $S^2 = 1.2$	(−303.28555)	(29.31)	0.00884	
UCCSD	aug-cc-PVDZ	TS1	−303.28439	14.93	1.72	616
		TS2, $S^2 = 1.3$	−303.27614	36.59	0.00279	

[a] The designations are the same as in Table 3. Unparenthesized numbers refer to TS2a; parenthesized numbers, to TS2b.

although the ratio of the rate constants for the two reaction pathways has a treasonable value ($k_1/k_2 \approx 10^2$) for all basis sets.

Table 4 presents the same data obtained by ab initio methods. The MP2 method, which is the most resource-demanding one, is unsuitable for describing TS2, because it leads to greatly overestimated energy of the open shells. Accordingly, the TS2 energy is heavily overestimated and, as a consequence, the activation energy is unrealistically high, making it impossible to analyze the k_1/k_2 ratio. The E_a value for the Criegee mechanism is fairly reasonable, and it is somewhat underestimated only with the aug-cc basis sets. The rate constants for the Criegee mechanism are in agreement with experimental data to an extent depending on the basis set. Therefore, provided that the basis set is rightly chosen, the MP2 method is usable in calculating the parameters of this pathway of the reaction. The QCISD method yields plausible values of the activation energy and k_1/k_2 ratio, but it overestimates the rate constant values themselves. The CCSD data—both the activation energy and the rate constants—are in full agreement with experimental data. The k_1/k_2 ratio is also quite plausible in this case. Thus, among the ab initio methods, the CCSD method is the most appropriate for solving the given problem.

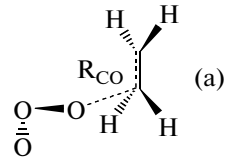

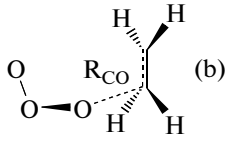

Fig. 2. TS structures in the reaction between ethylene and ozone occurring via nonconcerted addition: (a) *trans* TS2 (TS2a); (b) *cis* TS2 (TS2b).

The multi-configuration calculations also confirmed the existence of two mechanisms of the reaction. The kinetic data obtained by these calculations are listed in Table 5, which includes only the results obtained with active spaces not smaller than (10, 9), the minimum possible size for the given problem (see above). At smaller active space sizes, the calculated values of the activation energy and rate constant are indeed in conflict with the corresponding experimental data and seem unreasonable, so they are not included in Table 5. At sufficiently large active spaces, these parameters depend weakly on the space size and,

Table 5. TS1 and TS2 parameters calculated by MRMP2 multi-configuration methods

(n, m)	Basis set	TS optimization procedure	TS type	E, Ha	Parameter[a]		
					E_a, kJ/mol	k at 298 K, l mol^{-1} s^{-1}	k_1/k_2
(10, 9)	6-31+G**	(2)	TS1	−303.20037	25.7	2.13	10^4
			TS2	−303.18740	58.8	1.22×10^{-4}	
		(3)	TS1	−303.19663	24.1	1.93	10^4
			TS2	−303.19114	50.6	1.14×10^{-3}	
(10, 10)		(2)	TS1	−303.20115	20.3	21.14	10^5
			TS2	−303.18618	58.9	6.3×10^{-5}	
(14, 11)		(2)	TS1	−303.21313	24.8	1.70	10^5
			TS2	−303.19831	54.1	5.06×10^{-4}	
		(3)	TS1	−303.20853	23.4	2.63	10^3
			TS2	−303.19867	50.0	1.4×10^{-3}	
(14, 11)	aug-CC-PVDZ	(2)	TS1	−303.30478	16.7	20.1	6×10^3
			TS2	−303.29245	48.7	3.25×10^{-3}	

[a] The designations are the same as in Table 3.

in all cases, the activation energy for the Criegee mechanism is about 20 kJ/mol, which is in agreement with experimental data, and the activation energy for the DeMore mechanism is about 50 kJ/mol. The Criegee-to-DeMore rate constant ratio is within the 10^3–10^5 range, and this is again in agreement with the literature. On the whole, the results of the multi-configuration calculations are consistent with the data calculated in the single-determinant approximation (Tables 3, 4).

Note that the final result of the multi-configuration calculations depends only weakly on what geometry optimization method is used. At a fixed active space size, the rate constants obtained with optimization procedures (2) and (3) differ by a factor no larger than 3. This is further evidence of the adequacy of the methods used in this work and of the reliability of the results.

Thus, the calculations carried out in this study corroborate the earlier inference that the interaction of ozone with multiple bonds of organic compounds can proceed via two mechanisms, namely, concerted and nonconcerted additions. One of the reaction pathways is molecular, and the other is free-radical. This leads to certain difficulties in simulation of this interaction, because some methods are intended for molecules with closed shells, while others are intended for molecules with open shells. As was established earlier and confirmed in this study, ethylene ozonation occurs mainly via the Criegee mechanism, which is satisfactorily describable by the MP2 method. In principle, one can limit oneself to this method (or its analogue) in solving the given problem. However, in the interaction of ozone with molecules having electronegative (halogen), phenyl, or other substituents, the ratio of the rate constants of the reactions proceeding via the different pathways may vary [7], and this will pose the problem of describing both mechanisms at the same computational level. We have demonstrated that the Criegee and DeMore mechanisms can be described at one quantum chemical level using the B3LYP, PBE0, MRMP2, CCSD, and QCISD methods; however, the last two methods are very resource-demanding and are inappropriate for molecule that are more complex than ethylene. In view of this, for more complex molecules the Criegee mechanism can be simulated by the B3LYP, PBE0, MP2, and MRMP2 methods; the DeMore mechanism, by the B3LYP, PBE0, and MRMP2 methods.

REFERENCES

1. Razumovskii, S.D. and Zaikov, G.E., *Ozon i ego reaktsii s organicheskimi soedineniyami* (Ozone and Its Reactions with Organic Compounds), Moscow: Nauka, 1974.
2. Razumovskii, S.D. and Zaikov, G.E., *Usp. Khim.*, 1980, vol. 49, p. 2344.
3. Lunin, V.V., Popovich, M.P., and Tkachenko, S.N., *Fizicheskaya khimiya ozona* (Physical Chemistry of Ozone), Moscow: Mosk. Gos. Univ., 1998.
4. Criegee, R., *Angew. Chem.*, 1975, vol. 87, p. 765.
5. DeMore, W.B., *Int. J. Chem. Kinet.*, 1969, vol. 1, p. 209.
6. Cremer, D., Kraka, E., Crehuet, R., Anglada, J., and Grafenstain, J., *Chem. Phys. Lett.*, 2001, vol. 347, p. 268.
7. Denisov, E.T. and Krisyuk, B.E., *Khim. Fiz.*, 2007, vol. 26, no. 5, p. 34.

8. Floriano, W.B., Blaszkowski, S.R., and Nascimento, M.A.C., *J. Mol. Struct.*, 1995, vol. 335, p. 51.
9. Hiberty, P.C. and Leforestier, C., *J. Am. Chem. Soc.,* 1978, vol. 100, p. 2012.
10. Kahn, S.D., Hehre, W.J., and Pople, J.A., *J. Am. Chem. Soc.,* 1987, vol. 109, p. 1871.
11. Krisyuk, B.E., *Khim. Fiz.*, 2006, vol. 25, no. 6, p. 13.
12. Krisyuk, B.E., Maiorov, A.V., and Popov, A.A., *Khim. Fiz.*, 2007, vol. 26, no. 6, p. 16.
13. Chan, W.T. and Hamilton, I.P., *J. Chem. Phys.,* 2003, vol. 118, p. 1688.
14. Maiorov, A.V., Krisyuk, B.E., and Popov, A.A., *Khim. Fiz.*, 2007, vol. 26, no. 8, p. 22.
15. Maiorov, A.V., Krisyuk, B.E., and Popov, A.A., *Khim. Fiz.*, 2008, vol. 27, no. 9, p. 1.
16. Maiorov, A.V., Krisyuk, B.E., and Popov, A.A., *Khim. Fiz.*, 2008, vol. 27, no. 2, p. 62.
17. DeMore, W.B., Sander, S.P., Golden, D.M., Hampson, R.F., Kurylo, M.J., Howard, C.Y., Ravinshankara, A.R., Kolb, C.F., and Molina, M.J., *JPL Publication*, 1997, p. 97.
18. Frisch, M.J., Trucks, G.W., Schlegel, H.B., Scuseria, G.E., Robb, M.A., Cheeseman, J.R., Montgomery, J.A., Vreven, T., Kudin, K.N., Burant, J.C., Millam, J.M., Iyengar, S.S., Tomasi, J., Barone, V., Mennucci, B., Cossi, M., Scalmani, G., Rega, N., Petersson, G.A., Nakatsuji, H., Hada, M., Ehara, M., Toyota, K., Fukuda, R., Hasegawa, J., Ishida, M., Nakajima, T., Honda, Y., Kitao, O., Nakai, H., Klene, M., Li, X., Knox, J.E., Hratchian, H.P., Cross, J.B., Adamo, C., Jaramillo, J., Gomperts, R., Stratmann, R.E., Yazyev, O., Austin, A.J., Cammi, R., Pomelli, C., Ochterski, J.W., Ayala, P.Y., Morokuma, K., Voth, G.A., Salvador, P., Dannenberg, J.J., Zakrzewski, V.G., Dapprich, S., Daniels, A.D., Strain, M.C., Farkas, O., Malick, D.K., Rabuck, A.D., Raghavachari, K., Foresman, J.B., Ortiz, J.V., Cui, Q., Baboul, A.G., Clifford, S., Cioslowski, J., Stefanov, B.B., Liu, G., Liashenko, A., Piskorz, P., Komaromi, I., Martin, R.L., Fox, D.J., Keith, T., Al-Laham, M.A., Peng, C.Y., Nanayakkara, A., Challacombe, M., Gill, P.M.W., Johnson, B., Chen, W., Wong, M.W., Gonzalez, C., and Pople, J.A., *Gaussian 03, Revision C.02*, Wallingford, Conn.: Gaussian Inc., 2004.
19. http://www.msg.ameslab.gov/GAMESS/
20. Granovsky, A.A., PC GAMESS Version 7.0. http://classic.chem.msu.su/gran/gamess/index.html
21. Anglada, J.M. and Bofill, J.M., *Chem. Phys. Lett.*, 1995, vol. 243, p. 151.
22. Anglada, J.M., Crehuet, R., and Bofill, J.M., *Chem. Eur. J.*, 1999, vol. 5, p. 1809.
23. Ljubic, I. and Sabljic, A., *J. Phys. Chem.,* 2002, vol. 106, p. 4745.
24. Ignatov, S.K. http://ichem.unn.runnet.ru/tcg/Moltran.htm
25. Krisyuk, B.E., Maiorov, A.V., and Popov, A.A., *Khim. Fiz.*, 2003, vol. 22, no. 9, p. 3.